

Electrolyte-Resistant Dual Materials for the Synergistic Safety Enhancement of Lithium-Ion Batteries

Lien-Yang Chou,[#] Yusheng Ye,[#] Hiang Kwee Lee, Wenxiao Huang, Rong Xu, Xin Gao, Renjie Chen, Feng Wu, Chia-Kuang Tsung, and Yi Cui*

Cite This: *Nano Lett.* 2021, 21, 2074–2080

Read Online

ACCESS |

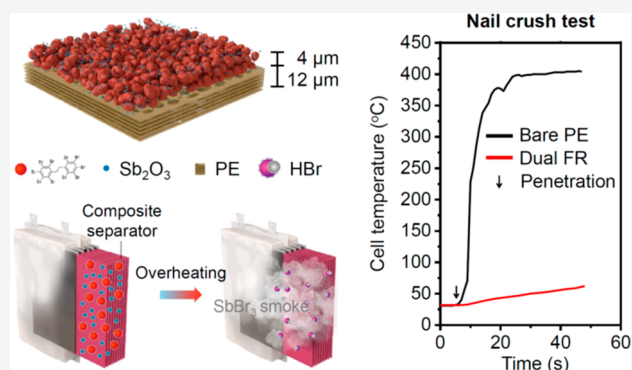
Metrics & More

Article Recommendations

Supporting Information

ABSTRACT: Safety issues associated with lithium-ion batteries are of major concern, especially with the ever-growing demand for higher-energy-density storage devices. Although flame retardants (FRs) added to electrolytes can reduce fire hazards, large amounts of FRs are required and they severely deteriorate battery performance. Here, we report a feasible method to balance flame retardancy and electrochemical performance by coating an electrolyte-insoluble FR on commercial battery separators. By integrating dual materials *via* a two-pronged mechanism, the quantity of FR required could be limited to an ultrathin coating layer (4 μm) that rarely influences electrochemical performance. The developed composite separator has a four-times better flame retardancy than conventional polyolefin separators in full pouch cells. Additionally, this separator can be fabricated easily on a large scale for industrial applications. High-energy-density batteries (2 Ah) were assembled to demonstrate the scaling of the composite separator and to confirm its enhanced safety through nail penetration tests.

KEYWORDS: Flame-retardant separator, fire extinguishing, ultrathin coating, lithium-ion battery



Lithium-ion batteries (LIBs) are highly desirable for portable electronics, electrical vehicles, drones, and other high-capacity battery-powered devices^{1,2} because of their design flexibility and high specific energy density. However, one of the major bottlenecks in the progress of LIBs is their potential safety hazards.^{3–5} LIBs use flammable internal components, such as organic electrolytes, separators, and electrodes,^{3,6,7} which aggravate thermal runaway in the case of overcharging and internal shorting. The exothermic reactions cause the internal temperature to increase rapidly, eventually leading to battery fires and even explosions, as reported worldwide in the last 10 years.^{3,8} The accidents have increased with the emergence of the electric vehicle market in 2015.⁸ Intensive research has been devoted to developing new functional components for improving the safety of LIBs, including studies on overcharging protection,⁹ thermally switchable current collectors,¹⁰ thermal shutdown separators,¹¹ separators with high thermal stability,^{12,13} solid-state electrolytes,¹⁴ and nonflammable liquid electrolytes.¹⁵ However, the risk of battery fire remains. Advances related to nonflammable electrolytes are restricted by high costs and limited electrochemical performance. Although methods related to battery components other than the electrolyte, such as automatic sensing of internal shorts¹⁶ or increasing the thermal stability,¹⁷

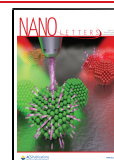
can improve the safety of LIBs, thermal runaway cannot be suppressed.

The addition of a flame retardant (FR) to flammable electrolytes¹² introduces preventive safety features into LIBs more effectively and economically¹⁸ and decreases the electrolyte flammability by increasing its flash point. Despite the potential to render organic electrolytes nonflammable, high concentrations of additives limit the LIB electrochemical performance due to increased electrolyte viscosity and reduced ionic conductivity. Separators containing FR may address this conundrum between the flammability and performance.^{19–23} However, poor mechanical performances and difficulties in scaled production for commercial applications have slowed the progress of this approach. Inspired by a ceramic-particle-coated separator, coating an electrolyte-insoluble FR directly on a commercialized separator is promising. While ceramics as metal hydroxides have shown FR properties, this approach has limited practical application in lithium-based batteries because

Received: December 3, 2020

Revised: January 15, 2021

Published: February 18, 2021



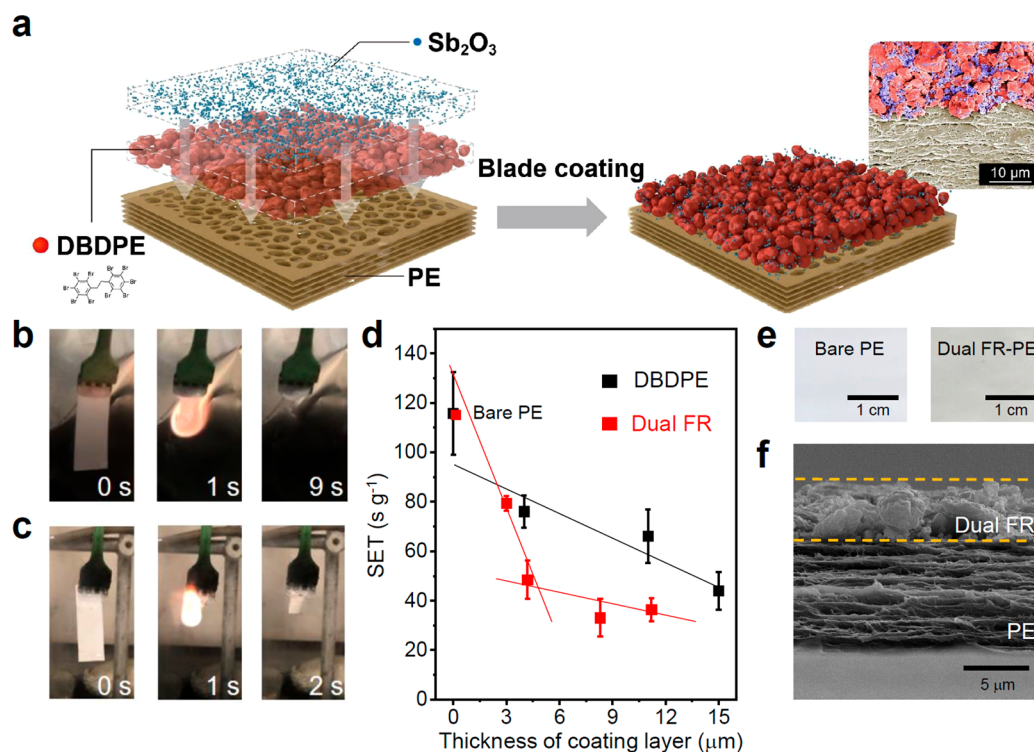


Figure 1. Flame retardancy and properties of FR composite separators. (a) Scheme illustrating the formation of the bilayered dual FR composite separator and the corresponding SEM image. Photographs recording the burning of (b) a bare PE separator and (c) an 8 μm dual-FR-coated separator. The separators were soaked in EC/DEC electrolyte before the burning experiments. (d) Self-extinguishing time (SET) of composite separators with different thicknesses of DBDPE and dual FR coating layers. (e) Photographs of bare PE and dual FR composite separators. (f) Cross-sectional SEM image of the FR composite separator.

the released water could react with the lithium metal violently, posing an even greater threat.^{24,25} The coating layer must be thick (20–30 μm)^{24,25} for achieving acceptable flame retardancy, but a thick coating layer increases the resistance of the separator and, thus, decreases the specific energy density of the LIB. The electrochemical instability of the coating layer is also problematic in terms of battery capacity degradation.²⁴ Batteries fabricated with a composite separator must pass industrial abuse procedures. Therefore, a small amount of potent, insoluble FR should be sufficient to achieve the desired flame retardancy, while maintaining the superior electrochemical performance of LIBs.

Here, we propose a considerably FR, electrochemically stable separator by coating the surface of a commercialized polyolefin separator with a layer of electrolyte-insoluble FR additives (Figure 1a). Two materials were chosen for a two-pronged approach to retard battery fires via a halogen radical scavenging mechanism, combined with dense SbBr_3 smoke to extinguish the flame by excluding oxygen. The novel composite separator has a bilayered structure: a layer consisting of dual components of insoluble FRs and commercial polyolefin as the coating backbone. In pouch cells, our separator shows efficient flame retardancy in burning tests, recovers from a short circuit, and prevents thermal runaway during nail penetration tests. Our unique separator coating process has several advantages over the conventional electrolyte–FR–additive strategy. First, electrolyte-insoluble FR additives should minimally affect the LIB electrochemical performance because they do not dissolve in the electrolyte to alter the intrinsic electrolyte properties. Second, the solid coating layer as a ceramic-particle coating¹³ enhances the thermal stability of the commercialized separator.

Third, the composite separator can inherit the favorable mechanical properties of the underlying polyolefin substrate and can be easily scaled for commercial usage.

As basic requirements, the solid FRs employed to form composite separators should be insoluble in the electrolyte and remain stable in the electrochemical environment. We used a brominated FR, viz. decabromodiphenyl ethane (DBDPE). DBDPE FRs neither contain ether bonds nor generate toxic dibenzofurans and dibenzo-*p*-dioxins,²⁶ thereby complying with the safety requirements set by the European Union.²⁷ DBDPE contains a high level of bromine (>81.5 wt %) and exhibits excellent flame retardancy even at low loading.²⁸ With a high bromine content, DBDPE has a high thermal stability²⁸ (degradation temperature >300 $^\circ\text{C}$) and extremely low solubility in most organic solvents²⁹ (<2 ppm); therefore, it was chosen as the FR to prove the proposed concept. Commercially available DBDPE powders of diameters 2–7 μm (Figure S1a) were coated onto 12 μm -thick conventional porous polyolefin separators with 10 wt % of polyvinylidene difluoride (PVDF) as the binder. Halogenated FRs have been reported to interfere with the gas-phase combustion process via a radical scavenging mechanism.³⁰ Halogen radicals generated from halogenated FRs can neutralize the $\text{H}\cdot$ and $\text{HO}\cdot$ radicals emitted by the chain reaction of the burning electrolyte. These much-less-active halogen radicals lower the rate of energy production and eventually extinguish the flame (Figure S1b). The thickness of the FR coating layer was adjusted to compare the flame retardancy and ionic conductivity at different thicknesses. The total thickness of the FR-coated separator was limited to <30 μm to avoid losing

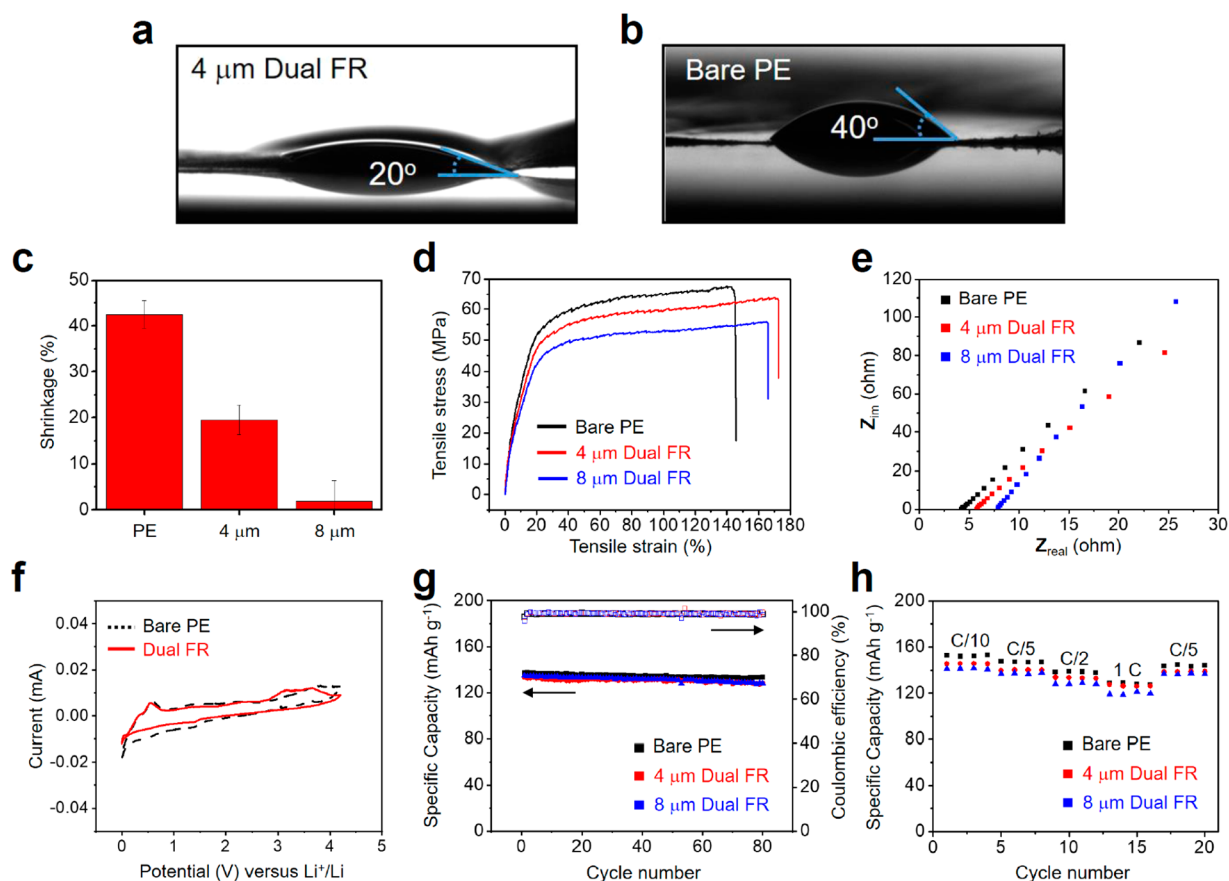


Figure 2. Characterization and electrochemical performance of dual FR composite separators. Contact angle images of the liquid electrolyte on the (a) dual FR composite and (b) bare PE separators. (c) Thermal shrinkage rate at 150 °C for 30 min and (d) mechanical properties of bare PE and dual FR composite separators of different thicknesses. (e) Nyquist plots obtained by EIS, (f) electrochemical stability window versus Li^+/Li^0 , (g) capacity retention, Coulombic efficiency, and (h) rate performance of bare PE and dual FR composite separators in coin cells.

the high energy density of LIBs. Therefore, we controlled the thickness of the coating layer between 4 and 15 μm .

The flame retardancy of the FR composite separators was tested with the electrolyte commonly used in LIBs, that is, 1.0 M LiPF_6 in ethylene carbonate (EC)/diethyl carbonate (DEC) (1:1, w/w). The flammability of the same amount of electrolyte was evaluated in the presence of a bare polyethylene (PE) separator and the FR-coated separator. As shown in Figure 1b and Video S1, the EC/DEC electrolyte was found to be highly flammable with the bare PE separator, burning over approximately 9 s compared with ~ 5 s with the FR-coated separator (Figure S2 and Video S2). Regarding flame retardancy, the self-extinguishing time (SET) of the electrolytes was measured to normalize the combustion time to the electrolyte mass for three repeated trials, and the SET decreased with increasing thickness of the coating layer (Figure 1d, black squares), confirming that the FR additives help reduce the flammability of the electrolyte.

We further optimized our method to achieve a thin coating (e.g., 4 μm) with considerable FR properties. We chose antimony trioxide (Sb_2O_3) which acts as a synergist with halogens, as an additive to DBDPE. Synergism occurs to generate antimony tribromide (SbBr_3), which forms dense white smoke to extinguish the flame by excluding oxygen^{31,32} (Figure S1c). By comparing coating layers of similar weights on PE separators with different amounts of DBDPE and Sb_2O_3 , we found that the flame retardancy enhanced significantly with increasing Sb_2O_3 content (Figure S3). Nevertheless, excess

Sb_2O_3 (more than 30%) would lead to reduced flame retardancy probably because Sb_2O_3 by itself is not an FR, as reported previously.³³ Therefore, an optimal ratio of DBDPE and Sb_2O_3 (3:1 ratio) achieved the best flame-retarding performance. The burning time of a 3:1 mixture of DBDPE and Sb_2O_3 , hereafter denoted as dual FR, was decreased to 2 s with a coating thickness of 8 μm (Figure 1c and Video S3). The dual FR coating significantly enhanced flame retardancy (2 s) compared to a pure DBDPE coating (5 s) at a much lower coating thickness (8 μm dual FR vs 11 μm DBDPE) (Figure 1c and Figure S2). We also analyzed the relationship between the SET and coating thickness of the dual FR coating layers. The results indicated that the SET decreases with increasing coating thickness (Figure 1d, red squares). This is similar to the behavior of the pure DBDPE coating; however, the decrease in SET noticeably reduces as the thickness exceeds 4 μm (the slope decreases from -17.7 to -1.5). This might be due to the limitation of the thermal trigger response time. The FRs require a specific time to accumulate heat that triggers the release of active materials ($\text{Br}\bullet$) and for synergism (formation of SbBr_3) to manifest.

The dual FR could be easily coated onto the separator as a homogeneous layer (Figure S4) for large-scale application. While the bare PE surface is highly reflective and white, that of the composite separator is matte white in appearance owing to the coating layer (Figure 1e). The cross-sectional and surface morphologies of a composite separator with a 4 μm -thick coating were observed by scanning electron microscopy

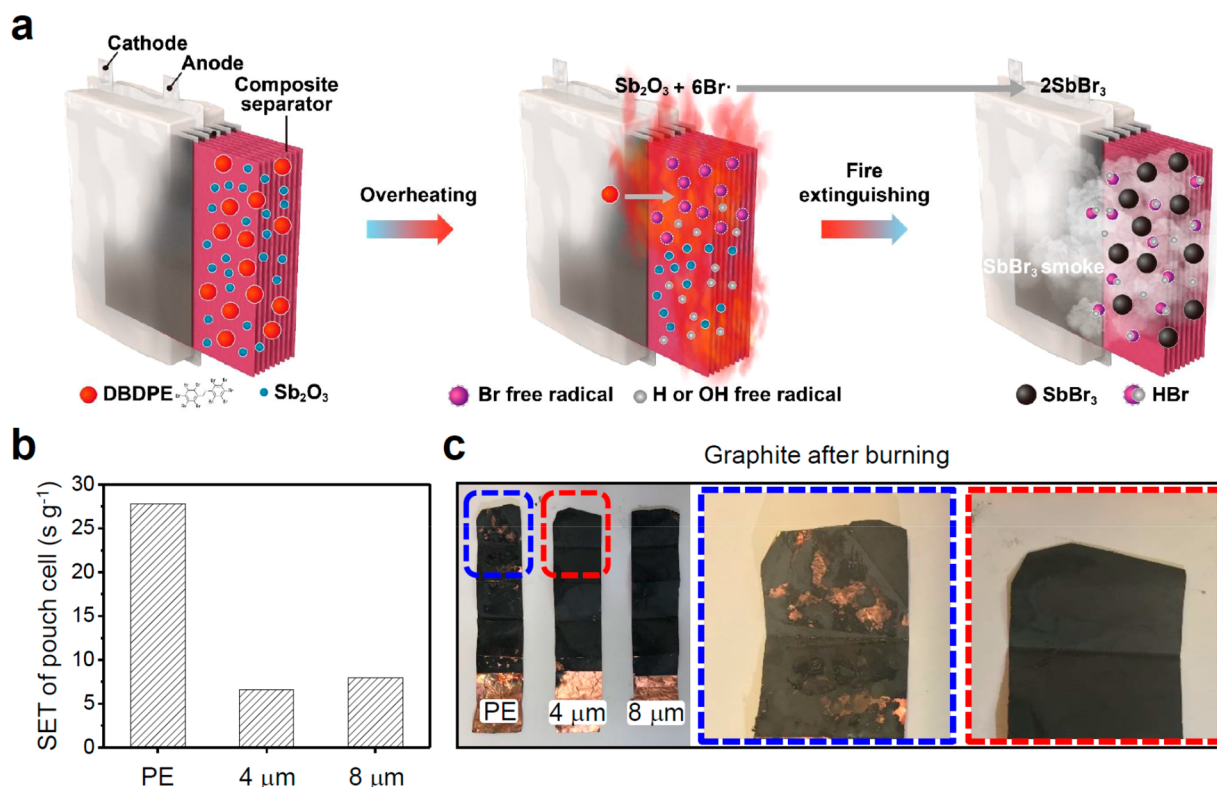


Figure 3. The burning test of full pouch cells. (a) Scheme illustrating the battery setup containing the FR composite separator. The flame-retarding mechanism is based on the bromide radical scavenging of the electrolyte combustion chain reaction combined with dense white smoke from SbBr_3 to snuff out the flame by excluding oxygen. (b) SET of pouch cells prepared using bare PE and dual FR composite separators of different coating thicknesses. (c) Photographs of graphite anodes after the burning test of pouch cells. The anode was assembled with bare PE (left) and with 4 μm (middle) and 8 μm (right) dual FR composite separators. The inset images are enlargements of the graphite anodes assembled with bare PE and the 4 μm dual FR composite separator.

(SEM) (Figure 1a,f). Although the particle size of the commercial DBDPE powder was 2–7 μm (Figure S1a), the large DBDPE particles could be filtered out through the blade coating process. The Sb_2O_3 particles were smaller than 1 μm (Figure S5); therefore, Sb_2O_3 particles could fill the interstitial spaces of DBDPE particles to form a homogeneous layer (Figure 1a). Hereafter, we compared 4 and 8 μm -thick coatings because both are thin and have similar FR properties. The objective was to determine if the thickness affects other physical properties.

Conventional polyolefin-type separators suffer from poor electrolyte affinity and low structural integrity when heated, leading to internal shorting and ultimately, thermal runaway.¹¹ The FR composite separators may function as ceramic coatings to enhance the hydrophilicity and thermal stability of commercialized separators. The electrolyte wettability was determined by contact angle measurements of the liquid electrolyte on the separators (Figure 2a,b). The contact angle of the electrolyte on the 4 μm -thick dual FR composite separator was 20° and that of the bare PE separator was 40°, which suggested that the coating layer increased the electrolyte wettability. A control experiment was also performed to measure the water contact angle on the separators (Figure S6a). The water contact angle was 120° for both separators, which illustrates the intrinsic hydrophobicity of their surfaces. The enhanced electrolyte wettability of the dual FR composite separator might result from the Sb_2O_3 component based on the wettability enhancement observed for conventional ceramic metal oxide coatings.¹¹

The thermal stability of the dual FR composite separators was evaluated after exposure to 150 °C for 30 min (Figure S6b), after which the shrinkage percentage was determined by measuring the dimensional changes (Figure 2c). The shrinkage percentage of the bare PE separator exceeded 40%, whereas that of the separator with the 4 μm -thick dual FR coating decreased to ~20%. With the 8 μm -thick coating layer, the shrinkage was even lower than 5%, thus the FR coating layer enhances the thermal stability of the separator.

Apart from having thermal stability, a separator must also be mechanically robust to bear the tension applied during battery assembly. The tensile strengths of the 4 and 8 μm -thick composite separators (total thickness with PE = 16 and 20 μm , respectively) were measured to be 63.8 and 56.0 MPa, respectively, slightly less than those of the bare PE separator (12 μm , 67.4 MPa), as shown in Figure 2d. The tensile strains of the 4 and 8 μm -thick composite separators, however, were 172% and 166%, respectively, while that of the bare PE separator was 145%. This might result from thicker membranes of composite separators, which is consistent with the total force measurements showing that thicker composite separators exhibit higher forces (Figure S6c).

Impedance measurements were performed on separators with different thicknesses of DBDPE coating layers (Figure S7a). Nyquist plots were obtained by electrochemical impedance spectroscopy (EIS) for both the bare PE and the FR-coated separators in the electrolyte, and the resistances of the FR composite separators did not change significantly. The corresponding resistance for the bare separator (~4 Ω) and

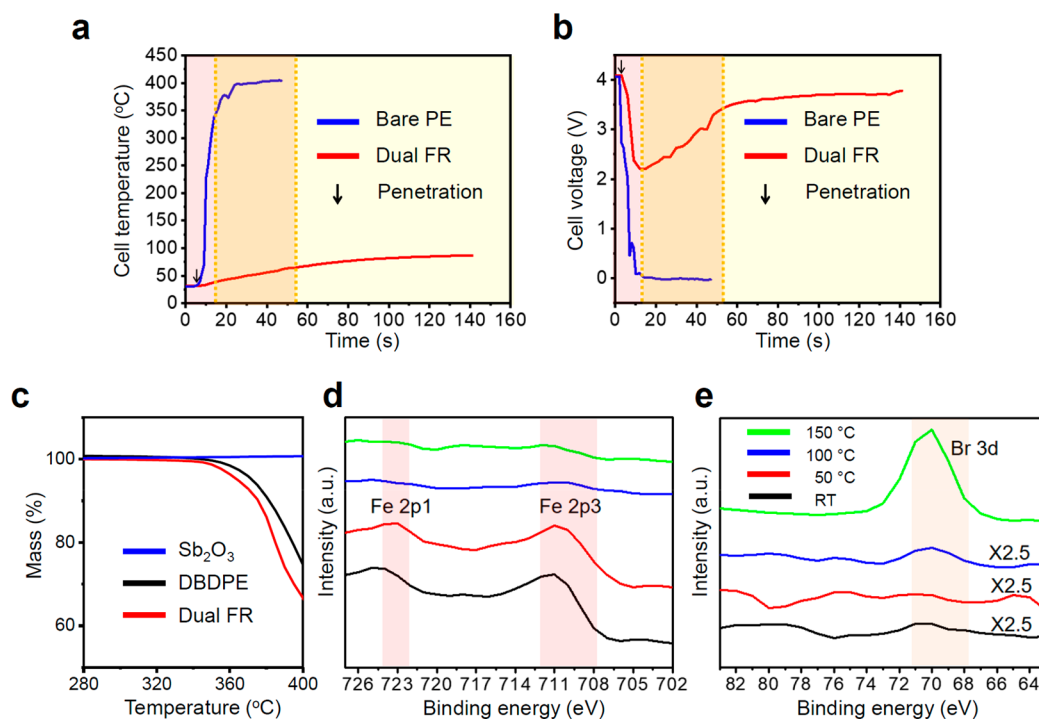


Figure 4. Nail penetration test of full pouch cells. (a) Temperature and (b) voltage profiles of pouch cells during the nail penetration test. (c) TGA of DBDPE, Sb_2O_3 , and dual FR. XPS analysis of (d) iron and (e) bromine on the surface of stainless steel after the thermal decomposition of dual FR at different temperatures.

that with the thickest coating ($15\ \mu\text{m}$, $\sim 9\ \Omega$) are shown in Figure S7b. The ionic conductivity of the dual FR composite separator was tested (Figure 2e). The resistances of the dual FR composite separators with coating thicknesses of 4 and $8\ \mu\text{m}$ were approximately 6 and $7.5\ \Omega$, respectively.

Next, the electrochemical stabilities of the dual FR composite separators were measured by cyclic voltammetry (CV) in a Li metal/separator + EC/DEC/stainless-steel setup at room temperature between 0 and 4.2 V vs Li^+/Li^0 at $1.0\ \text{mV s}^{-1}$ (Figure 2f). The CV curve of the composite separator ($4\ \mu\text{m}$ dual FR) is similar to that of the commercial PE separator, confirming the composite separators' high stability in the LIB working environment in the electrochemical window up to 4.2 V vs Li^+/Li^0 . The dual FR composite separators also afforded remarkable battery performance (Figure 2g). Using lithium cobalt oxide (LCO) as the cathode and Li metal as the anode, all half-cells prepared with different composite separators exhibited similar Coulombic efficiencies and good reversibility. Compared with the bare PE separator, the discharge capacities of both the 4 and $8\ \mu\text{m}$ -thick composite separators were slightly lower, but they still showed a reversibility similar to that of bare PE. The composite separators showed slightly lower discharge capacities than the bare separator, but still yielded a good rate capability (Figure 2h). There was little difference in specific capacity only under a higher rate (1 C), suggesting that the slightly lower ionic conductivity decreases the specific capacity only negligibly. Collectively, these flame retardancy and electrochemical evaluations highlight that the designed composite separators can extinguish electrolyte fires, while maintaining the battery performance almost identical to that of the bare separator.

To test the flame retardancy of the full cells, a whole battery was assembled with graphite/separator + electrolyte/cathode for burning tests (Figure 3a). An 85 mAh pouch cell was

prepared with $600\ \mu\text{L}$ of the electrolyte and sealed in an Ar environment. The whole-cell flame retardancy test was performed after 24 h of resting to ensure that the cell was fully soaked with the electrolyte (Figure S8a). The burning time of the pouch cell with the bare PE separator was $\sim 20\ \text{s}$ (Video S4), while those for the $4\ \mu\text{m}$ -thick and $8\ \mu\text{m}$ -thick composite separators were $\sim 5\ \text{s}$ (Videos S5 and S6, respectively). Both the dual FR composite separators reduced the SET of the pouch cell to a value approximately four times less than that of the cell with bare PE (Figure 3b). The graphite from the bare PE pouch cell showed distinct damage from burning; however, the graphite from the pouch cells with the composite separators appeared normal, indicating that the damage was contained with a short burning time (Figure 3c). For both pouch cells with composite separators, some electrolyte remained after burning, implying that the composite separators are highly effective in extinguishing battery fires.

We further investigated the ability of our composite separators to enhance LIB safety during an electrical short by nail penetration test (Figure S8b) to simulate the thermal runaway process caused by mechanical impact on the battery and/or penetration of undesirable conductive materials through the separator (such as Li dendrites). Here, we chose the $4\ \mu\text{m}$ -thick dual FR composite separator for the analysis. Pouch cells (2 Ah) were assembled with graphite/separator + EC/DEC/LCO and fully charged, and nails were driven through the cells. The bare PE assembled pouch cell generated a significant amount of smoke within 5 s following nail penetration (Figure S9a and Video S7) and the cell temperature reached $228\ ^\circ\text{C}$ in 5 s (Figure 4a) and continuously increased to $400\ ^\circ\text{C}$ in another 20 s. With our composite separator (Figure S9b and Video S8), no smoke was observed, and the temperature increased slowly and eventually reached a plateau at approximately $90\ ^\circ\text{C}$ after 2 min of nail

penetration (Figure 4a). The voltage of the pouch cell with bare PE immediately dropped to zero after nail penetration (Figure 4b). In contrast, that of the composite separator initially decreased from ~4 to 2.2 V and gradually reverted to 3.8 V after 60 s, possibly due to the formation of a passive surface layer on the nail caused by the reaction of DBDPE and Sb_2O_3 on the locally heated nail when a massive discharge current passes through it.

Thermogravimetric analysis (TGA) was performed to study the reaction of DBDPE and Sb_2O_3 (Figures 4c and Figure S10). The TGA curve of DBDPE shows a weight loss starting at ~345 °C. Under the same heating conditions, the TGA curve of pure Sb_2O_3 shows a weight gain, originating from the oxidation of Sb_2O_3 to a higher oxidized state (e.g., Sb_2O_5).³⁴ However, the TGA curve of the dual FR shows a weight loss starting at ~310 °C, much lower than that of pure DBDPE. To determine if a passive surface layer formed from the reaction of the dual FR additives, heated stainless-steel samples were contacted with the dual FR coating layer. After cooling to room temperature, the surfaces of the stainless-steel samples were analyzed by XPS. The iron peaks (Fe 2P1 and Fe 2P3) decreased in intensity at temperatures higher than 100 °C, while the bromine signal (Br 3d) appeared at nearly the same temperature above 100 °C (Figure 4d,e). However, no antimony signal (Sb 3d5) was detected even at 150 °C (Figure S11). These observations suggest that a bromine-containing layer formed on the stainless-steel surface at temperatures higher than 100 °C, but the trace reaction could not be observed by TGA.

To further understand the effects of the passive surface layer formation on nail shorting, we performed a COMSOL simulation of the battery behavior upon nail penetration (Figure S12a) using the electrochemical–thermal coupled model in COMSOL Multiphysics 5.3 (for details see the SI). The local temperature increase from Joule heating was simulated by the heat transfer model, in which the time-dependent temperature distribution in the batteries was solved simultaneously with the electrochemical self-discharge (Figure S12b). The simulated cell voltage and local temperature after nail penetration agreed with the experimental results further confirming passive surface layer formation (Figure S12c,d).

A thin-layer coating of an electrolyte-insoluble, high-performance FR on commercialized polyolefin separators significantly enhances the safety of LIBs and maintains their electrochemical performance. We demonstrated a thin-layer coating of an FR composite for the separator by applying two flame-retarding mechanisms by a feasible inorganic particle-coating method. The dual FR composite separator can be fabricated easily on a large scale, and it was proven to yield an acceptable electrochemical performance. Furthermore, the low cost and commercially available raw materials used here might expand the scope of practical production. Herein, we report a simple concept for improving the safety of LIBs and offers a perspective on industrial applications for their further design and development.

■ ASSOCIATED CONTENT

SI Supporting Information

The Supporting Information is available free of charge at <https://pubs.acs.org/doi/10.1021/acs.nanolett.0c04568>.

Materials, methods, supporting figures, and supporting table (PDF)

Videos S1–S8 (ZIP)

■ AUTHOR INFORMATION

Corresponding Author

Yi Cui – Department of Materials Science and Engineering, Stanford University, Stanford, California 94305, United States; Stanford Institute for Materials and Energy Sciences, SLAC National Accelerator Laboratory, Menlo Park, California 94025, United States; orcid.org/0000-0002-6103-6352; Email: yicui@stanford.edu

Authors

Lien-Yang Chou – Department of Materials Science and Engineering, Stanford University, Stanford, California 94305, United States; orcid.org/0000-0001-8171-1346

Yusheng Ye – Department of Materials Science and Engineering, Stanford University, Stanford, California 94305, United States; orcid.org/0000-0001-9832-2478

Hiang Kwee Lee – Department of Materials Science and Engineering, Stanford University, Stanford, California 94305, United States

Wenxiao Huang – Department of Materials Science and Engineering, Stanford University, Stanford, California 94305, United States

Rong Xu – Department of Materials Science and Engineering, Stanford University, Stanford, California 94305, United States

Xin Gao – Department of Materials Science and Engineering, Stanford University, Stanford, California 94305, United States; orcid.org/0000-0001-5360-0796

Renjie Chen – Beijing Key Laboratory of Environmental Science and Engineering, School of Materials Science and Engineering, Beijing Institute of Technology, Beijing 100081, China; orcid.org/0000-0002-7001-2926

Feng Wu – Beijing Key Laboratory of Environmental Science and Engineering, School of Materials Science and Engineering, Beijing Institute of Technology, Beijing 100081, China

Chia-Kuang Tsung – Department of Chemistry, Merkert Chemistry Centre, Boston College, Boston, Massachusetts 02467, United States; orcid.org/0000-0002-9410-565X

Complete contact information is available at: <https://pubs.acs.org/10.1021/acs.nanolett.0c04568>

Author Contributions

[#]These authors contributed equally to this work.

Notes

The authors declare no competing financial interest.

■ ACKNOWLEDGMENTS

The work was supported by the Assistant Secretary for Energy Efficiency and Renewable Energy, Office of Vehicle Technologies of the U.S. Department of Energy under the Battery Materials Research (BMR) Program. L.-Y.C. acknowledges Dr. Kai Liu, Dr. Hao Chen, and Dr. Xin Xiao for discussions and technical support.

■ REFERENCES

- (1) Tarascon, J. M.; Armand, M. Issues and challenges facing rechargeable lithium batteries. *Nature* **2001**, *414* (6861), 359–367.
- (2) Goodenough, J. B.; Park, K.-S. The Li-Ion Rechargeable Battery: A Perspective. *J. Am. Chem. Soc.* **2013**, *135* (4), 1167–1176.

- (3) Wang, Q.; Ping, P.; Zhao, X.; Chu, G.; Sun, J.; Chen, C. Thermal runaway caused fire and explosion of lithium ion battery. *J. Power Sources* **2012**, *208*, 210–224.
- (4) Balakrishnan, P. G.; Ramesh, R.; Prem Kumar, T. Safety mechanisms in lithium-ion batteries. *J. Power Sources* **2006**, *155* (2), 401–414.
- (5) Jansen, A. N.; Kahaian, A. J.; Kepler, K. D.; Nelson, P. A.; Amine, K.; Dees, D. W.; Vissers, D. R.; Thackeray, M. M. Development of a high-power lithium-ion battery. *J. Power Sources* **1999**, *81–82*, 902–905.
- (6) Yao, X. L.; Xie, S.; Chen, C. H.; Wang, Q. S.; Sun, J. H.; Li, Y. L.; Lu, S. X. Comparative study of trimethyl phosphite and trimethyl phosphate as electrolyte additives in lithium ion batteries. *J. Power Sources* **2005**, *144* (1), 170–175.
- (7) Zhang, S. S. A review on electrolyte additives for lithium-ion batteries. *J. Power Sources* **2006**, *162* (2), 1379–1394.
- (8) Feng, X.; Ouyang, M.; Liu, X.; Lu, L.; Xia, Y.; He, X. Thermal runaway mechanism of lithium ion battery for electric vehicles: A review. *Energy Storage Mater.* **2018**, *10*, 246–267.
- (9) Haregewoin, A. M.; Wotango, A. S.; Hwang, B.-J. Electrolyte additives for lithium ion battery electrodes: progress and perspectives. *Energy Environ. Sci.* **2016**, *9* (6), 1955–1988.
- (10) Chen, Z.; Hsu, P.-C.; Lopez, J.; Li, Y.; To, J. W. F.; Liu, N.; Wang, C.; Andrews, S. C.; Liu, J.; Cui, Y.; Bao, Z. Fast and reversible thermoresponsive polymer switching materials for safer batteries. *Nat. Energy* **2016**, *1* (1), 15009.
- (11) Zhang, S. S. A review on the separators of liquid electrolyte Li-ion batteries. *J. Power Sources* **2007**, *164* (1), 351–364.
- (12) Liu, K.; Liu, Y.; Lin, D.; Pei, A.; Cui, Y. Materials for lithium-ion battery safety. *Sci. Adv.* **2018**, *4* (6), No. eaas9820.
- (13) Lee, H.; Yanilmaz, M.; Toprakci, O.; Fu, K.; Zhang, X. A review of recent developments in membrane separators for rechargeable lithium-ion batteries. *Energy Environ. Sci.* **2014**, *7* (12), 3857–3886.
- (14) Famprikis, T.; Canepa, P.; Dawson, J. A.; Islam, M. S.; Masquelier, C. Fundamentals of inorganic solid-state electrolytes for batteries. *Nat. Mater.* **2019**, *18* (12), 1278–1291.
- (15) Wang, Q.; Jiang, L.; Yu, Y.; Sun, J. Progress of enhancing the safety of lithium ion battery from the electrolyte aspect. *Nano Energy* **2019**, *55*, 93–114.
- (16) Wu, H.; Zhuo, D.; Kong, D.; Cui, Y. Improving battery safety by early detection of internal shorting with a bifunctional separator. *Nat. Commun.* **2014**, *5* (1), 5193.
- (17) Liu, K.; Zhuo, D.; Lee, H.-W.; Liu, W.; Lin, D.; Lu, Y.; Cui, Y. Extending the Life of Lithium-Based Rechargeable Batteries by Reaction of Lithium Dendrites with a Novel Silica Nanoparticle Sandwiched Separator. *Adv. Mater.* **2017**, *29* (4), 1603987.
- (18) Dagger, T.; Rad, B. R.; Schappacher, F. M.; Winter, M. Comparative Performance Evaluation of Flame Retardant Additives for Lithium Ion Batteries - I. Safety, Chemical and Electrochemical Stabilities. *Energy Technol.* **2018**, *6* (10), 2011–2022.
- (19) Liu, K.; Liu, W.; Qiu, Y.; Kong, B.; Sun, Y.; Chen, Z.; Zhuo, D.; Lin, D.; Cui, Y. Electrospun core-shell microfiber separator with thermal-triggered flame-retardant properties for lithium-ion batteries. *Sci. Adv.* **2017**, *3* (1), No. e1601978.
- (20) Zhang, J.; Yue, L.; Kong, Q.; Liu, Z.; Zhou, X.; Zhang, C.; Xu, Q.; Zhang, B.; Ding, G.; Qin, B.; Duan, Y.; Wang, Q.; Yao, J.; Cui, G.; Chen, L. Sustainable, heat-resistant and flame-retardant cellulose-based composite separator for high-performance lithium ion battery. *Sci. Rep.* **2015**, *4*, 3935.
- (21) Zeng, G.; Zhao, J.; Feng, C.; Chen, D.; Meng, Y.; Boateng, B.; Lu, N.; He, W. Flame-Retardant Bilayer Separator with Multifaceted van der Waals Interaction for Lithium-Ion Batteries. *ACS Appl. Mater. Interfaces* **2019**, *11* (29), 26402–26411.
- (22) Schadeck, U.; Kyrgyzbaev, K.; Zettl, H.; Gerdes, T.; Moos, R. Flexible, Heat-Resistant, and Flame-Retardant Glass Fiber Non-woven/Glass Platelet Composite Separator for Lithium-Ion Batteries. *Energies* **2018**, *11* (4), 999.
- (23) Yim, T.; Park, M.-S.; Woo, S.-G.; Kwon, H.-K.; Yoo, J.-K.; Jung, Y. S.; Kim, K. J.; Yu, J.-S.; Kim, Y.-J. Self-Extinguishing Lithium Ion Batteries Based on Internally Embedded Fire-Extinguishing Microcapsules with Temperature-Responsiveness. *Nano Lett.* **2015**, *15* (8), 5059–5067.
- (24) Yeon, D.; Lee, Y.; Ryou, M.-H.; Lee, Y. M. New flame-retardant composite separators based on metal hydroxides for lithium-ion batteries. *Electrochim. Acta* **2015**, *157*, 282–289.
- (25) Jung, B.; Lee, B.; Jeong, Y.-C.; Lee, J.; Yang, S. R.; Kim, H.; Park, M. Thermally stable non-aqueous ceramic-coated separators with enhanced nail penetration performance. *J. Power Sources* **2019**, *427*, 271–282.
- (26) Watanabe, I.; Sakai, S.-I. Environmental release and behavior of brominated flame retardants. *Environ. Int.* **2003**, *29* (6), 665–682.
- (27) Ranz, A.; Maier, E.; Trampitsch, C.; Lankmayr, E. Microwave-assisted extraction of decabromodiphenylether from polymers. *Talanta* **2008**, *76* (1), 102–106.
- (28) Xu, X.-N.; Chen, N.; Xu, W.-Y.; Wu, X.-C.; Zheng, L.-F. Research on the properties of flame retarded polymer materials using decabromodiphenyl ethane. *Fire Saf. Sci.* **2005**, *15* (2), 1001–1004.
- (29) Kierkegaard, A.; Björklund, J.; Fridén, U. Identification of the Flame Retardant Decabromodiphenyl Ethane in the Environment. *Environ. Sci. Technol.* **2004**, *38* (12), 3247–3253.
- (30) Troitzsch, J. H. Overview of Flame Retardants: Fire and Fire Safety, Markets and Applications, Mode of Action and Main Families. Role in Fire Gases and Residues. *Chem. Today* **1998**, *16*, 7.
- (31) Yu, L.; Wang, W.; Xiao, W. The effect of decabromodiphenyl oxide and antimony trioxide on the flame retardation of ethylene-propylene-diene copolymer/polypropylene blends. *Polym. Degrad. Stab.* **2004**, *86* (1), 69–73.
- (32) Chen, X.-S.; Yu, Z.-Z.; Liu, W.; Zhang, S. Synergistic effect of decabromodiphenyl ethane and montmorillonite on flame retardancy of polypropylene. *Polym. Degrad. Stab.* **2009**, *94* (9), 1520–1525.
- (33) La Rosa, A. D.; Recca, A.; Carter, J. T.; McGrail, P. T. An oxygen index evaluation of flammability on modified epoxy/polyester systems. *Polymer* **1999**, *40* (14), 4093–4098.
- (34) Schwarzmann, E.; Rumpel, H.; Berndt, W. Synthese von Diantimonpentoxid Sb₂O₅/Synthesis of Diantimony Pentoxide Sb₂O₅. *Z. Naturforsch., B: J. Chem. Sci.* **1977**, *32* (6), 617–618.